

Covariant calculation of the properties of f_2 mesons in a generalized Nambu–Jona-Lasinio model

L. S. Celenza, Bo Huang, Huangsheng Wang, and C. M. Shakin*

Department of Physics and Center for Nuclear Theory, Brooklyn College of the City University of New York, Brooklyn, New York 11210

(Received 22 February 1999; published 2 August 1999)

We use our covariant model of light-meson structure to study the f_2 tensor mesons. Our model is a generalized Nambu–Jona-Lasinio (NJL) model that includes a relativistic model of confinement. For the study of tensor mesons, we extend the NJL model to include interactions that contain gradients of the quark fields. There are two such terms requiring the introduction of two additional coupling constants for the model. We find a good fit to the experimentally determined states. We obtain ten states below 2 GeV, while there are eight states in the data tables with energies less than 2 GeV, if we include the recently found $f_J(1750)$ in our list of f_2 mesons. We find f_2' states of $s\bar{s}$ structure at 1551, 1745, and 1767 MeV. The first two of these states have nodeless wave functions and may be identified with the $f_2'(1525)$ and the $f_J(1750)$, if $J=2$ for the new state. (The state at 1767 MeV is a $2S$ $s\bar{s}$ state, which may mix with the 1745 MeV state to some degree.) Our analysis suggests a new classification for nonets of radially excited states that is based upon our relativistic model of light-meson structure. [S0556-2813(99)06608-X]

PACS number(s): 14.40.Cs, 12.39.Fe, 12.39.Ki

I. INTRODUCTION

In this work we continue our study of a generalized Nambu–Jona-Lasinio (NJL) model [1] that includes a relativistic model of confinement. In previous work we have studied the radial excitations of the pion including pseudoscalar–axial-vector mixing [2]. We have also studied ϕ - ω mixing and η - η' mixing. For the η - η' system we have included both singlet-octet mixing and pseudoscalar–axial-vector mixing [3]. More recently, we have studied the scalar, pseudoscalar, vector, and axial-vector nonets with quite satisfactory results [4].

A natural extension of these calculations is to consider tensor mesons. As we will see, we have to further generalize the NJL model to include short-range interactions that affect the states of such mesons. These new interactions contain gradients of the quark fields and may be thought of as being part of a more comprehensive expansion of the quark-antiquark interaction than that which appears in the standard form of the SU(3)-flavor NJL Lagrangian.

In this work we will study the f_2 mesons, which have $I^G(J^{PC})=0^+(2^{++})$, where I is the isospin and G is the G parity. To further motivate this study, we refer to Table I, where the states of the f_2 mesons are listed [5]. [We have not listed the $f_J(1710)$, although it is possible that state has $J=2$.] We see that there are a large number of states, with eight states below 2.0 GeV. This large number of states creates a problem for the standard constituent quark model [6]. This matter is discussed on p. 557 of Ref. [5], where it is suggested that the $f_2(1270)$ and $f_2'(1525)$ are probably the two 1^3P_2 $q\bar{q}$ states of the quark model. It is remarked that there are a large number of possible non- $q\bar{q}$ candidates with $J^{PC}=2^{++}$: $f_2(1430)$, $f_2(1520)$, $f_J(1710)$, $f_2(1810)$,

$f_2(2010)$, $f_2(2300)$, and $f_2(2340)$. It is stated that the $f_2(1810)$ is likely to be the 2^3P_2 state and the three f_2 mesons above 2 GeV could be the 2^3P_2 $s\bar{s}$, 1^3F_2 $s\bar{s}$, and 1^3P_2 $s\bar{s}$ states. As we will see, our fully relativistic calculation can readily account for the full range of states seen below 2 GeV. That is, in part, due to the fact the spacing of levels in the relativistic confinement potential is quite different from that in the quark model [6], with the $1S$, $2S$, and $3S$ $n\bar{n}$ states and the $1S$ and $2S$ $s\bar{s}$ states bound by the relativistic confining field at energies less than 2 GeV. [Here $n\bar{n}$ stands for the $(u\bar{u}+d\bar{d})/\sqrt{2}$ states.] Since the search for exotic, hybrid, or gluonium states is an important part of meson spectroscopy [6], we believe our formalism will be of value in identifying states of $q\bar{q}$ structure that can then be eliminated in the search for non- $q\bar{q}$ states.

TABLE I. Experimental values for the mass and width of f_2 mesons [5]. The small dots in the first column denote confirmed f_2 states as given in Ref. [5]. Reference [16] describes the observation of a $f_J(1750)$.

Meson	Mass (MeV)	Width (MeV)
$\cdot f_2(1270)$	1275 ± 5	185 ± 20
$f_2(1430)$	≈ 1430	
$\cdot f_2'(1525)$	1525 ± 5	76 ± 10
$f_2(1565)$	1565 ± 20	170 ± 40
$f_2(1640)$	1638 ± 6	99_{-24}^{+28}
$f_J(1750)$	1770 ± 20	200 ± 50
$f_2(1810)$	1815 ± 12	195 ± 22
$f_2(1950)$	1950 ± 15	250 ± 50
$\cdot f_2(2010)$	2011_{-76}^{+62}	202_{-62}^{+67}
$f_2(2150)$	$\sim 2150-2226$	250
$f_J(2220)$	2225 ± 6	38_{-13}^{+15}
$\cdot f_2(2300)$	2297 ± 28	149 ± 41
$\cdot f_2(2340)$	2339 ± 55	319_{-69}^{+81}

*Electronic address: CASBC@CUNYVM.CUNY.EDU

The organization of our work is as follows. In Sec. II we discuss some of the successes and limitations of our model and compare our approach to other models. In Sec. III we exhibit additional interaction terms that allow us to treat 2^{++} states in our generalized NJL model. In Sec. IV, we describe the T matrix used in our study of the f_2 mesons. This T matrix allows for a general study of singlet-octet mixing: however, in this work we limit our investigation to a model with “ideal mixing.” In Sec. V we present the results of our numerical calculations, while Sec. VI contains some further discussion and conclusions.

II. GENERALIZED NJL MODEL WITH A COVARIANT MODEL OF CONFINEMENT

In order to understand the merits and the limitations of our model, we will discuss the relation of our model to two models to be found in the literature. These are the extensively studied constituent quark model [6] and the work of Münz and collaborators [7–11].

As we have seen in our earlier work, our model provides quite good fits to the full range of light-meson spectra in terms of a number of phenomenological parameters. In the few cases that our fit is not particularly good, we find that the physical meson state appears very close to a threshold for a two-meson decay channel. An example is the $a_0(980)$, which lies directly below the threshold for the $K\bar{K}$ channel at 990 MeV. In this case we overestimate the mass of the $a_0(980)$ by 80 MeV. This suggests that a study of the influence of the decay channels in modifying the theoretical values of the masses of various mesons is in order.

An attempt to study the full range of light meson states is reviewed by Godfrey and Napolitano [6]. Their review contains a description of results obtained using a “relativized” version of the potential models that are highly successful in obtaining fits the spectra of heavy mesons. Since that model does not describe chiral symmetry breaking, it is not suited to the description of the pseudoscalar nonet of states. (One can use a spin-spin interaction to obtain the correct pion mass, with the consequence that the ρ mass is not given correctly [6].) Also, the nonrelativistic nature of the model leads to a poor description of the density of states in the low-energy spectrum. For example, in Ref. [6], we find two 3P_2 states and one 3F_2 states below 2 GeV in a study of tensor mesons. As discussed in the Introduction, we find ten f_2 states below 2.0 GeV. The first seven of these states can be put into correspondence with the first seven experimentally determined states. Problems in obtaining the correct number states in a nonrelativistic formulation can also be seen when we study pseudoscalar–axial-vector mixing for the pion and its radial excitations, as well as for the η - η' system of states. For example, in the meson rest frame we may discuss states with vertex structure of the form $i\gamma_5$ or $\gamma^0\gamma_5$. That immediately doubles the number of states we have to consider in a fully relativistic formalism. In our study of the pion, the states in the confining field appear as doublets, which are then split when the NJL interaction is included. This feature leads to an interesting interpretation of

the data in the region of the $\pi(1300)$, which is presented in Ref. [2]. In that work, the covariant nature of our formalism is particularly important, since we calculate meson decay amplitudes at one-loop order. For example, in the decays $\pi' \rightarrow \rho + \pi$, or $\pi' \rightarrow \sigma + \pi$, the final-state mesons have finite momentum, requiring a covariant model of the confining vertex for a consistent description [2]. While we have made extensive calculations of light-meson spectra, we have only calculated meson decay amplitudes in a few cases. Our recent work has included a description of the decays $\pi \rightarrow \gamma + \gamma$, $\eta \rightarrow \gamma + \gamma$, and $\eta' \rightarrow \gamma + \gamma$. We have found that our description of pseudoscalar–axial-vector mixing is quite important in obtaining a consistent picture of these decay rates [12,13].

Another model which may be used to make a comprehensive fit to the properties of light mesons is a model based upon the six-quark interaction of the 't Hooft model that has its origin in the study of instantons [8]. The model described in Ref. [8] also includes an (instantaneous) linear confining potential, which is used when solving the Salpeter equation. However, the model is not covariant, since only the timelike part of the potential, which is proportional to $\gamma^0(1)\gamma^0(2)$, is used, rather than the $\gamma^\mu(1)\gamma_\mu(2)$ form that we have used in our work. The model of Ref. [8] can provide a good fit to various spectra: however, the predictions for the decay widths are quite poor. Another choice of parameters yields good values for the decay rates: however, the fit to the spectra is then poor [8].

We have found that it is useful to neglect confinement for the $\pi(138)$ in our Minkowski-space calculations, since the properties of the pion are very sensitive to small violations of chiral symmetry that appear in our analysis. On the other hand, we have studied the pion using our model in a Euclidean-space calculation, where it is easy to maintain chiral symmetry (in the absence of a current-quark mass matrix). In that work, we found that the Goldstone theorem was satisfied, with the pion as the Goldstone boson [14].

Some discussion of our choice of parameters is in order. We define the parameters G_S and G_V in Eq. (3.1). In addition, there is the “string tension” κ and a Minkowski-space momentum cutoff Λ_3 , which is usually chosen so that the pion decay constant f_π is given correctly. We begin by fixing $m_u = m_d = 0.364$ GeV. That is the value used in the extensive calculations of Vogl and Weise [1]. We then chose G_V and κ so that the mass of the ω and the mass of the first radial excitation of the ω are given correctly. At that point, we fix $m_s = 0.565$ GeV, so that the mass of the ϕ meson is reproduced using the value of κ already determined. Finally, we fix G_S by fitting the mass of the $K(495)$. (When studying the η - η' system [4], we used a smaller value of G_S in singlet states to take into account effects due to the coupling to gluonic intermediate states. We found that to be a superior phenomenological scheme, as compared to the use of the 't Hooft interaction, which affects both singlet and octet states [1].) Once the parameters of the model are fixed by fitting the energies of the $\omega(782)$, $\omega(1420)$, $K(495)$, and $\phi(1020)$, we find that the model has significant predictive power. For example, the masses of the $K^*(892)$, $K_0^*(1430)$, and $a_1(1260)$ are predicted correctly [4]. In the present work, we

introduce two additional parameters that are defined in Eq. (3.9). The values are determined so as to yield a good fit to the masses of the f_2 mesons.

III. TENSOR MESONS IN A GENERALIZED NJL MODEL

We begin by introducing the Lagrangian of the generalized NJL model that we have studied in the past [2–4]:

$$\begin{aligned} \mathcal{L} = & \bar{q}(i\partial - m^0)q + \frac{G_S}{4} \sum_{i=0}^8 [(\bar{q}\lambda^i q)^2 + (\bar{q}i\gamma_5\lambda^i q)^2] \\ & - \frac{G_V}{4} \sum_{i=0}^8 [(\bar{q}\gamma^\mu\lambda^i q)^2 + (\bar{q}\gamma^\mu\gamma_5\lambda^i q)^2] + \mathcal{L}_{\text{conf}}. \end{aligned} \quad (3.1)$$

Here the λ_i ($i=1, \dots, 8$) are the Gell-Mann matrices and $\lambda_0 = \sqrt{2}/3I$, with I being the unit matrix in flavor space. Further, $m^0 = \text{diag}(m_u^0, m_d^0, m_s^0)$ is the current quark mass matrix and $\mathcal{L}_{\text{conf}}$ represents the Lagrangian of our confinement model. (We use Lorentz-vector confinement, so that our Lagrangian exhibits chiral symmetry in the absence of a quark mass matrix.)

The standard NJL Lagrangian that is exhibited as part of Eq. (3.1) describes interactions in the scalar, pseudoscalar, vector, and axial-vector nonets. If we are to study the f_2 tensor mesons, we need to add various interactions to the Lagrangian of Eq. (3.1). That may be done in a manner that preserves the chiral symmetry of the Lagrangian.

We now consider the following interaction Lagrangian:

$$\begin{aligned} \mathcal{L}_Q^{\text{int}} = & g_{T_1} \sum_{a=0}^8 \{ [\bar{q}\lambda^a (3\partial^\mu\partial^\nu - g^{\mu\nu}\square)q] \\ & \times [\bar{q}\lambda_a (3\tilde{\partial}_\mu\tilde{\partial}_\nu - g_{\mu\nu}\tilde{\square})q] + \text{c.p.} \}, \end{aligned} \quad (3.2)$$

where ‘‘c.p.’’ stands for the ‘‘chiral partner’’ of the first term. Rather than work with Eq. (3.2), we go directly to the momentum-space interaction and consider two new terms. We define two dimensionless tensors

$$Q^{\mu\nu}(k) = \frac{3\hat{k}^\mu\hat{k}^\nu - \tilde{g}^{\mu\nu}\hat{k}^2}{-2\hat{k}^2} \quad (3.3)$$

and

$$P^{\mu\nu}(k) = \frac{\hat{k}^\mu\gamma_{\perp,k}^\nu + \hat{k}^\nu\gamma_{\perp,k}^\mu}{\sqrt{-\hat{k}^2}}. \quad (3.4)$$

[See Eqs. (3.5)–(3.7).] Note that $Q_\mu^\mu = P_\mu^\mu = 0$. Since we have chosen to make these tensors dimensionless by dividing by \hat{k}^2 in Eq. (3.3) and $(-\hat{k}^2)^{1/2}$ in Eq. (3.4), $Q^{\mu\nu}$ is not in direct correspondence with Eq. (3.2): however, Eq. (3.2) could be modified to achieve that correspondence. We may also write a coordinate-space version of Eq. (3.4), but we will not need that form of the interaction Lagrangian for the present work.

We define

$$\hat{k}^\mu(P) = k^\mu - \frac{(k \cdot P)P^\mu}{P^2}, \quad (3.5)$$

$$\gamma_{\perp,k}^\mu = \hat{\gamma}^\mu - \frac{\hat{k}^\mu\hat{k}}{\hat{k}^2}, \quad (3.6)$$

$$\hat{\gamma}^\mu = \gamma^\mu - P^\mu P/P^2, \quad (3.7)$$

and

$$\tilde{g}^{\mu\nu} = g^{\mu\nu} - \frac{P^\mu P^\nu}{P^2}. \quad (3.8)$$

Note that $\hat{k} \cdot P = \gamma_{\perp,k} \cdot P = \hat{k} \cdot \gamma_{\perp,k} = 0$. We will carry out our analysis in the meson rest frame, where $\vec{P} = 0$ and $\hat{k}^\mu = [0, \vec{k}]$. Thus we only need to use the spatial components of the tensors Q^{ij} and P^{ij} . However, it is best to maintain the complete relativistic notation, since calculations are simpler in that case.

We now extend the NJL momentum-space interaction to include two attractive interactions and write

$$\begin{aligned} V_T(P, k', k) = & -\frac{G_{T_1}}{4} Q^{\mu\nu}(k') g_{\mu\nu\alpha\beta} Q^{\alpha\beta}(k) \\ & - \frac{G_{T_2}}{4} P^{\mu\nu}(k') g_{\mu\nu\alpha\beta} P^{\alpha\beta}(k). \end{aligned} \quad (3.9)$$

Here $g_{\mu\nu\alpha\beta}$, which depends upon P^μ , is defined to be

$$g^{\mu\nu\alpha\beta} = \frac{1}{2} \left\{ \tilde{g}^{\mu\alpha}\tilde{g}^{\nu\beta} + \tilde{g}^{\mu\beta}\tilde{g}^{\nu\alpha} - \frac{2}{3}\tilde{g}^{\mu\nu}\tilde{g}^{\alpha\beta} \right\}. \quad (3.10)$$

Note that $g^{\mu\nu}_{\alpha\beta} g^{\alpha\beta\rho\sigma} = g^{\mu\nu\rho\sigma}$. Following our standard procedure [2–4], we introduce equations for the tensor vertex functions:

$$\begin{aligned} \bar{\Gamma}_{T_1}^{\mu\nu}(P, k) = & Q^{\mu\nu}(k) - i \int \frac{d^4 k'}{(2\pi)^4} [\gamma^\rho S(P/2 + k') \\ & \times \bar{\Gamma}_{T_1}^{\mu\nu}(P, k') S(-P/2 + k') \gamma_\rho V^C(k - k')] \end{aligned} \quad (3.11)$$

and

$$\begin{aligned} \bar{\Gamma}_{T_2}^{\mu\nu}(P, k) = & P^{\mu\nu}(k) - i \int \frac{d^4 k'}{(2\pi)^4} [\gamma^\rho S(P/2 + k') \\ & \times \bar{\Gamma}_{T_2}^{\mu\nu}(P, k') S(-P/2 + k') \gamma_\rho V^C(k - k')]. \end{aligned} \quad (3.12)$$

The Dirac matrices γ^ρ and γ_ρ appear since we use Lorentz-vector confinement. [Equations (3.11) and (3.12) may be generalized to describe a quark and antiquark of different constituent mass values. However, for our study of the f_2

mesons, we only need these equations for $n\bar{n}$ or $s\bar{s}$ states. The more general form is needed in a study of strange mesons.]

We proceed as usual and define four functions for the case $\vec{P}=0$:

$$\begin{aligned} & \Lambda^{(+)}(\vec{k})\bar{\Gamma}_{T_1}^{\mu\nu}(P,k)\Lambda^{(-)}(-\vec{k}) \\ &= \Gamma_{T_1,1}^{+-}(P,k)Q^{\mu\nu}\Lambda^{(+)}(\vec{k})\Lambda^{(-)}(-\vec{k}) \\ &+ \Gamma_{T_1,2}^{+-}(P,k)\Lambda^{(+)}(\vec{k})P^{\mu\nu}\Lambda^{(-)}(-\vec{k}) \end{aligned} \quad (3.13)$$

and

$$\begin{aligned} & \Lambda^{(+)}(\vec{k})\Gamma_{T_2}^{\mu\nu}(P,k)\Lambda^{(-)}(-\vec{k}) \\ &= \Gamma_{T_2,1}^{+-}(P,k)Q^{\mu\nu}\Lambda^{(+)}(\vec{k})\Lambda^{(-)}(-\vec{k}) \\ &+ \Gamma_{T_2,2}^{+-}(P,k)\Lambda^{(+)}(\vec{k})P^{\mu\nu}\Lambda^{(-)}(-\vec{k}). \end{aligned} \quad (3.14)$$

The equations that may be used to determine the four functions defined in Eqs. (3.13) and (3.14) are given in the Appendix.

We now need to define a number of vacuum polarization functions. We write

$$\begin{aligned} -iJ_{QQ,ab}^{\mu\nu\alpha\beta}(P) &= -n_c \text{Tr} \int \frac{d^4k}{(2\pi)^4} [\lambda_a iS(P/2+k) \\ &\times \bar{\Gamma}_{T_1}^{\mu\nu}(P,k) iS(-P/2+k) Q^{\alpha\beta}(k) \lambda_b], \end{aligned} \quad (3.15)$$

where a and b are 0 or 8 in an analysis of singlet-octet mixing. We also define

$$\begin{aligned} -iJ_{PQ,ab}^{\mu\nu\alpha\beta}(P) &= -n_c \text{Tr} \int \frac{d^4k}{(2\pi)^4} [\lambda_a iS(P/2+k) \\ &\times \bar{\Gamma}_{T_1}^{\mu\nu}(P,k) iS(-P/2+k) P^{\alpha\beta}(k) \lambda_b], \end{aligned} \quad (3.16)$$

with a corresponding definition of $-iJ_{PQ,ab}^{\mu\nu\alpha\beta}$. We also write

$$\begin{aligned} -iJ_{PP,ab}^{\mu\nu\alpha\beta}(P) &= -n_c \text{Tr} \int \frac{d^4k}{(2\pi)^4} [\lambda_a iS(P/2+k) \\ &\times \Gamma_{T_2}^{\mu\nu}(P,k) iS(-P/2+k) P^{\alpha\beta}(k) \lambda_b]. \end{aligned} \quad (3.17)$$

Now we define

$$J_{QQ,ab}^{\mu\nu\alpha\beta}(P) = g^{\mu\nu\alpha\beta} J_{ab}^{QQ}(P^2), \quad (3.18)$$

$$J_{PQ,ab}^{\mu\nu\alpha\beta}(P) = g^{\mu\nu\alpha\beta} J_{ab}^{PQ}(P^2), \quad (3.19)$$

and

$$J_{PP,ab}^{\mu\nu\alpha\beta}(P) = g^{\mu\nu\alpha\beta} J_{ab}^{PP}(P^2), \quad (3.20)$$

with $J_{ab}^{QP}(P^2) = J_{ab}^{PQ}(P^2)$.

We obtain, for a quark of mass m_u and with $k=|\vec{k}|$,

$$J_u^{QQ}(P^2) = -\frac{3}{10\pi^2} n_c \int^{\Lambda_3} k^2 dk \frac{k^2}{E^2(k)} \frac{\Gamma_{T_1,1}^{+-}(P,k)}{P^0 - 2E_u(k)}, \quad (3.21)$$

where $E_u(k) = [k^2 + m_u^2]^{1/2}$. [Note that the various functions $\Gamma^{+-}(P,k)$ depend upon the mass of the quark.] There is a corresponding equation for $J_s^{QQ}(P^2)$. The values of $J_{ab}^{QP}(P^2)$ are obtained from knowledge of $J_u^{QQ}(P^2)$ and $J_s^{QQ}(P^2)$.

We find that

$$J_u^{PP}(P^2) = -\frac{4}{5\pi^2} n_c \int^{\Lambda_3} k^2 dk \frac{\Gamma_{T_2,2}^{+-}(P,k)}{P^0 - 2E_u(k)}, \quad (3.22)$$

$$J_u^{QP}(P^2) = -\frac{4}{5\pi^2} n_c \int^{\Lambda_3} k^2 dk \frac{\Gamma_{T_1,2}^{+-}(P,k)}{P^0 - 2E_u(k)}, \quad (3.23)$$

etc. In obtaining these results we have used the relation $g_{\mu\nu\alpha\beta}g^{\mu\nu\alpha\beta} = 5$ and have neglected small terms proportional to $[P^0 + 2E(k)]^{-1}$.

IV. T MATRICES FOR THE STUDY OF f_2 MESONS

We now construct the matrices that enable us to study singlet-octet and $Q_{\mu\nu}(k) - P_{\mu\nu}(k)$ mixing. [We remark that the latter mixing occurs due to the nonzero values of $J_{ab}^{QP}(P^2) = J_{ab}^{PQ}(P^2)$.] We define the matrix

$$J(P^2) = \begin{pmatrix} J_{00}^{QQ} & J_{08}^{QQ} & J_{00}^{QP} & J_{08}^{QP} \\ J_{80}^{QQ} & J_{88}^{QQ} & J_{80}^{QP} & J_{88}^{QP} \\ J_{00}^{PQ} & J_{08}^{PQ} & J_{00}^{PP} & J_{08}^{PP} \\ J_{80}^{PQ} & J_{88}^{PQ} & J_{80}^{PP} & J_{88}^{PP} \end{pmatrix}, \quad (4.1)$$

where all the elements depend upon P^2 . We also put the T matrix into a 4×4 matrix form, using the basis vector

$$\Phi^{\mu\nu}(k) = \begin{pmatrix} Q^{\mu\nu}(k)\lambda_0 \\ Q^{\mu\nu}(k)\lambda_8 \\ P^{\mu\nu}(k)\lambda_0 \\ P^{\mu\nu}(k)\lambda_8 \end{pmatrix} \quad (4.2)$$

and its transpose. Thus we write

$$\hat{T}(P^2, k', k) = \Phi_{\mu\nu}^T(k') \hat{T}^{\mu\nu\alpha\beta}(P^2) \Phi_{\alpha\beta}(k), \quad (4.3)$$

where $\hat{T}^{\mu\nu\alpha\beta}(P) = g^{\mu\nu\alpha\beta} \tilde{T}(P)$. Here $\tilde{T}(P^2)$ is also a 4×4 matrix.

We also define the matrix

$$G = - \begin{pmatrix} G_{T_1} & 0 & 0 & 0 \\ 0 & G_{T_1} & 0 & 0 \\ 0 & 0 & G_{T_2} & 0 \\ 0 & 0 & 0 & G_{T_2} \end{pmatrix}. \quad (4.4)$$

We then solve the matrix equation

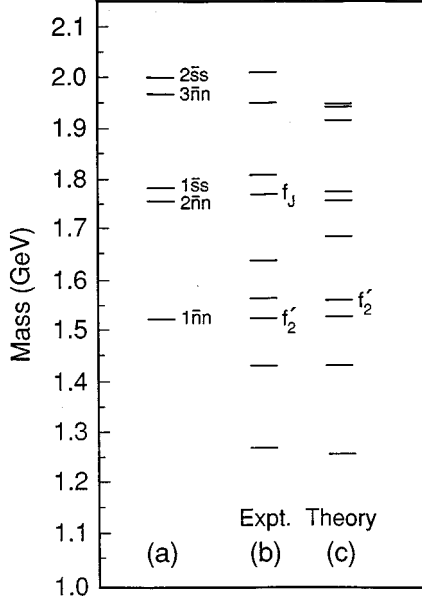


FIG. 1. (a) The levels in the confining field are shown for $m_u = m_d = 0.364$ GeV, $m_s = 0.565$ GeV, $\kappa = 0.055$ GeV², and $\mu = 0.010$ GeV. Here $\bar{n}n = (\bar{u}u + \bar{d}d)/\sqrt{2}$. (b) Experimental values of the masses of the f_2 mesons. The $f_2'(1525)$ is assumed to have a $s\bar{s}$ configuration and it is possible that the $f_2(1750)$ is such a state [16]. (c) Theoretical mass values are shown for $G_{T_1} = 47.00$ GeV⁻² and $G_{T_2} = 6.80$ GeV⁻². The mass values are 1254, 1429, 1527, 1551, 1685, 1745, 1767, 1913, 1939, and 1943 MeV.

$$[1 + GJ(P^2)]\tilde{T}(P^2) = G \quad (4.5)$$

and write

$$\tilde{T}(P^2) = [1 + GJ(P^2)]^{-1}G. \quad (4.6)$$

TABLE II. Values of the mass, g , g' , and the mixing angles for the lowest five states obtained in this work. Here ideal mixing is seen, as expected. Additional $s\bar{s}$ states are found at 1745, 1767, and 1943 MeV and additional $(u\bar{u} + d\bar{d})$ states are found at 1913 and 1939 MeV. The six $(u\bar{u} + d\bar{d})$ states and the four $s\bar{s}$ states listed above correspond to the five states shown in Fig. 1(a), which have a degeneracy factor of 2. Here $m_u = 0.364$ GeV, $m_s = 0.565$ GeV, $\kappa = 0.055$ GeV², $\Lambda_3 = 0.622$ GeV, and $\mu = 0.010$ GeV [2–4]. The two new parameters introduced in this work are $G_{T_1} = 47.00$ GeV⁻² and $G_{T_2} = 6.80$ GeV⁻².

Mass (MeV)	Type	g	g'	$\hat{\theta}$ (deg)	$\tilde{\theta}$ (deg)
1254	$n\bar{n}$ 1S	7.82	-1.48	-35.26	-35.26
1429	$n\bar{n}$ 1S	4.62	2.12	-35.26	-35.26
1527	$n\bar{n}$ 2S	0.931	0.612	-35.26	-35.26
1551	$s\bar{s}$ 1S	-3.56	1.85	54.79	54.79
1685	$n\bar{n}$ 2S	0.972	-0.808	-35.26	-35.26

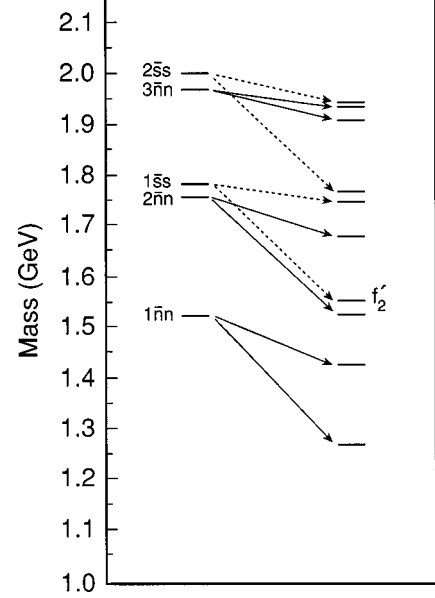


FIG. 2. The states of Fig. 1(a) are put into correspondence with the states of Fig. 1(c). The dotted lines refer to the $s\bar{s}$ states. For each doublet, a state that is mainly 3P_2 lies lower in energy than the other member of the doublet, which is mainly of 3F_2 character.

Theoretical values for the masses of the f_2 mesons may be determined by finding the values of P^2 for which $\tilde{T}(P^2)$ is singular. Near a singularity of $\tilde{T}(P^2)$ we may write

$$\langle k' | \tilde{T}(P^2) | k \rangle = -F^{\mu\nu}(k') \frac{g_{\mu\nu\alpha\beta}}{P^2 - m_i^2} F^{\alpha\beta}(k), \quad (4.7)$$

where m_i^2 is the theoretical value of the squared mass of one of our f_2 mesons. Here we have defined the form factor

$$F^{\mu\nu}(k) = gQ^{\mu\nu}(k)[\cos \hat{\theta}\lambda_0 - \sin \hat{\theta}\lambda_8] + g'P^{\mu\nu}(k)[\cos \tilde{\theta}\lambda_0 - \sin \tilde{\theta}\lambda_8]. \quad (4.8)$$

We may include confinement effects in the numerator of the T matrix [15] if we replace $F^{\alpha\beta}(k)$ by

TABLE III. Quark-antiquark states bound in the confining field at energies above 2 GeV. (See Fig. 2.) Here $m_u = 0.364$ GeV, $m_s = 0.565$ GeV, and $\kappa = 0.055$ GeV².

Principal quantum number	$n\bar{n}$ Mass (GeV)	$s\bar{s}$ Mass (GeV)
3		2.205
4	2.155	2.373
5	2.319	2.517
6	2.455	2.653
7	2.570	2.760
8		2.860
9		2.970

$$F_c^{\mu\nu}(k) = g\bar{\Gamma}_{T_1}^{\mu\nu}(P,k)[\cos\hat{\theta}\lambda_0 - \sin\hat{\theta}\lambda_8] \\ + g'\bar{\Gamma}_{T_2}^{\mu\nu}(P,k)[\cos\tilde{\theta}\lambda_0 - \sin\tilde{\theta}\lambda_8], \quad (4.9)$$

where $P^2 = m_i^2$. The presence of the confinement vertices $\bar{\Gamma}_{T_1}^{\mu\nu}(P,k)$ and $\bar{\Gamma}_{T_2}^{\mu\nu}(P,k)$ allows us to show that the T matrix is represented by bound states only, if the potential V^C is absolutely confining [15]. Recall that equations for $\bar{\Gamma}_{T_1}^{\mu\nu}(P,k)$ and $\bar{\Gamma}_{T_2}^{\mu\nu}(P,k)$ were presented in Eqs. (3.11) and (3.12).

If the matrix G is of the form given in Eq. (4.4), we find ideal mixing. If a state has the structure $(\bar{u}u + \bar{d}d)/\sqrt{2}$, the mixing angles are $\hat{\theta} = \tilde{\theta} = -35.26^\circ$ and, for a $\bar{s}s$ state, $\hat{\theta} = \tilde{\theta} = 54.74^\circ$. Deviations from ideal mixing can be obtained if we use different interactions for singlet and octet states. Such effects may be found if one takes into account the coupling of states through the gluon field, a feature which only affects the strength of the interaction in singlet states.

V. RESULTS OF NUMERICAL CALCULATIONS

As noted earlier, the spectrum of states may be obtained by studying the singularities of the T matrix. Results of our calculations are found in Fig. 1 and Table II. In Fig. 1(a) we show the positions of the bound states in the confining field in the absence of the NJL interaction. The $1S \bar{n}n$ state is at 1520 MeV, with the $2S$ and $3S$ states at about 1755 and 1970 MeV, respectively. The $1S$ and $2S s\bar{s}$ states are at 1790 and 1998 MeV. These states all have a degeneracy factor of 2, since they may be associated with the vertex governed by either $Q^{\mu\nu}$ or $P_{\mu\nu}$. Since the NJL forces are attractive, we expect to find at least ten states below 2 GeV. We show these ten states in Fig. 1. (See Fig. 2 and Table III.)

The $1S \bar{n}n$ state gives rise to two states at 1254 and 1429 MeV, if we take $G_{T_1} = 47.0 \text{ GeV}^{-2}$ and $G_{T_2} = 6.8 \text{ GeV}^{-2}$. The next state at 1527 MeV seen in Fig. 1(c) originates from the $2S \bar{n}n$ state. The fourth state at 1551 MeV, is a $1S s\bar{s}$ state and may be identified with the $f_2'(1525)$. (We see that we have overestimated the energy of that state by about 25 MeV.) There are two f_2' states at 1745 and 1767 MeV. (See Fig. 2.) The first of these states, which is nodeless, may be identified with the $f_J(1750)$ if $J^{PC} = 2^{++}$ for that state [16]. (The $2S s\bar{s}$ state at 1767 MeV may mix with the $1S$ state at 1745 MeV to some degree.)

The $2S \bar{n}n$ state bound in the confining field gives rise to the states at 1524 and 1685 MeV. The second of these states may be identified with the $f_2(1640)$. We note that the two $2S \bar{n}n$ states at 1524 and 1685 MeV in Table II have small values of g and g' when compared with the three $1S$ states listed in the table. That is as expected, since the coupling constants for meson-quark coupling (g and g') decrease rapidly with increase of the number of nodes in the meson wave function. [We remark that the phase of the form factor, $F^{\mu\nu}(k)$ or $F_c^{\mu\nu}(k)$, is arbitrary: however, the relative phase of g and g' is meaningful.]

VI. DISCUSSION

As may be seen in Fig. 1, we predict one or two more states than are seen in experiment. That suggests that there is little evidence in our study for non- $q\bar{q}$ states below 2 GeV. Since some of the states shown in Fig. 1(c) are quite close in energy, there could be a good deal of additional configuration mixing, since the states can be coupled to each other via their decay channels. However, the first four states appear reasonably well isolated from the other groupings and their characterization may survive further coupling interactions such as that mentioned above.

We have also remarked that the spacing of levels in the confining field is radically different than that obtained from a harmonic oscillator potential. For example, in our model, states that differ by a single node in the wave function are separated by about 225 MeV. [See Fig. 1(a).] However, if we consider the $1S n\bar{n}$ state at about 1520 MeV and subtract $2m_u = 728$ MeV, we are left with an excitation in the potential of approximately 800 MeV, a value that may be compared to the 225 MeV level separation mentioned above. We conclude that the covariant confinement model places the states in the confining field [Fig. 1(a)] in a quite satisfactory arrangement, so that the introduction of two new terms in the short-range (NJL) interaction brings the theoretical spectrum into overall agreement with the f_2 states obtained from experiment.

ACKNOWLEDGMENTS

This work is supported in part by a grant from the National Science Foundation and by the PSC-CUNY Faculty Research Award Program.

APPENDIX

In this appendix we present equations that may be solved to obtain $\Gamma_{T_1,i}^{+-}$, $\Gamma_{T_1,2}^{+-}$, $\Gamma_{T_2,1}^{+-}$, and $\Gamma_{T_2,2}^{+-}$. These equations are obtained from Eqs. (3.11) and (3.12). One method that may be used is to multiply $\bar{\Gamma}^{\mu\nu}(P,k)$ from the right by $\Lambda^{(-)}(-\vec{k})$ and from the left by $\Lambda^{(+)}(\vec{k})$. One can then multiply from the left by either $Q^{\mu\nu}$ or $P_{\mu\nu}$ and then form the trace of both sides of the equation. We find, with $i=1$ or 2 ,

$$\Gamma_{T_1,i}^{+-}(P,k) = C_i - \sum_{j=1}^2 \int \frac{dk'}{(2\pi^2)} t_{ij}(k,k',x) \\ \times \left(\frac{m}{E(k')} \right)^2 \frac{V^C(\vec{k}-\vec{k}')}{P^0 - 2E(k')} \Gamma_{T_1,j}^{+-}(P,k'). \quad (A1)$$

Here $C_1 = 1$ and $C_2 = 0$. With $x = \cos \theta$, we have

$$t_{11}(k,k',x) = - \left[2 \left(\frac{k'}{m} \right)^2 + \frac{k'x}{k} \right] P_2(x), \quad (A2)$$

$$t_{12}(k,k',x) = \left[\frac{E(k')}{m} \right]^2 2x(1-x^2) \frac{m}{k}, \quad (A3)$$

$$t_{21}(k, k', x) = \frac{3}{4} x(1-x^2) \frac{k'}{m}, \quad (\text{A4})$$

and

$$t_{22}(k, k', x) = - \left[\frac{E(k')}{m} \right]^2 \left[x^3 + \frac{kk'}{E(k)E(k')} P_2(x) \right]. \quad (\text{A5})$$

In Eqs. (A2) and (A5), $P_2(x)$ is a Legendre function. Also, $k = |\vec{k}|$, $k' = |\vec{k}'|$ in all the equations given above. Corresponding equations for $\Gamma_{T_2,1}^{+-}$ and $\Gamma_{T_2,2}^{+-}$ are obtained by replacing C_i by D_i where $D_1=0$ and $D_2=1$. We then see that the homogenous equations for the various Γ^{+-} are the same. Therefore, $\Gamma_{T_1,1}^{+-}$, $\Gamma_{T_1,2}^{+-}$, $\Gamma_{T_2,1}^{+-}$, and $\Gamma_{T_2,2}^{+-}$ have singularities at the same energies.

-
- [1] For reviews of the NJL model, see S. P. Klevansky, *Rev. Mod. Phys.* **64**, 649 (1992); U. Vogl and W. Weise, *Prog. Part. Nucl. Phys.* **27**, 195 (1991).
- [2] L. S. Celenza, Bo Huang, and C. M. Shakin, *Phys. Rev. C* **59**, 1041 (1999).
- [3] Bo Huang, Xiang-Dong Li, and C. M. Shakin, *Phys. Rev. C* **58**, 3648 (1998).
- [4] L. S. Celenza, Bo Huang, Huangsheng Wang, and C. M. Shakin, *Phys. Rev. C* **60**, 025202 (1999).
- [5] Particle Data Group, R. M. Barnett *et al.*, *Phys. Rev. D* **54**, 1 (1996).
- [6] A review of light-meson spectroscopy is given in S. Godfrey and J. Napolitano, *Rev. Mod. Phys.* (submitted), hep-ph/9811410, 1998.
- [7] C. R. Münz, J. Resag, B. C. Metsch, and H. R. Petry, *Nucl. Phys. A* **578**, 418 (1994); J. Resag, C. R. Münz, B. C. Metsch, and H. R. Petry, *ibid.* **A578**, 397 (1994).
- [8] C. R. Münz, *Nucl. Phys. A* **609**, 364 (1996).
- [9] C. Ritter, B. C. Metsch, C. R. Münz, and H. R. Petry, *Phys. Lett. B* **380**, 431 (1996).
- [10] E. Klempt, B. C. Metsch, C. R. Münz, and H. R. Petry, *Phys. Lett. B* **361**, 160 (1995).
- [11] C. R. Münz, B. C. Metsch, and H. R. Petry, *Phys. Rev. C* **52**, 2110 (1995).
- [12] L. S. Celenza, Bo Huang, and C. M. Shakin, *Phys. Rev. C* **59**, 1700 (1999).
- [13] L. S. Celenza, Bo Huang, and C. M. Shakin, *Phys. Rev. C* **59**, 2814 (1999).
- [14] L. S. Celenza, Xiang-Dong Li, and C. M. Shakin, *Phys. Rev. C* **55**, 1492 (1997).
- [15] L. S. Celenza, Bo Huang, and C. M. Shakin, *Phys. Rev. C* **59**, 1030 (1999).
- [16] T. Van Rhee, *Acta Phys. Pol. B* **29**, 3401 (1998); S. Braccini, contribution to LEAP98, Villasimus, Italy, 1998, hep-ex/9811017.